

X-523-66-13

NASA TM X- 55448

PHASE STABILITY ASPECTS OF THE GSFC BORESIGHT RF SOURCES

7 JANUARY 1966

GPO PRICE \$ _____

CFSTI PRICE(S) \$ _____

Hard copy (HC) 1.00

Microfiche (MF) .50

7 653 July 65



GODDARD SPACE FLIGHT CENTER
GREENBELT, MARYLAND

FACILITY FORM 602

N66 24394

(ACCESSION NUMBER)

15
(PAGES)

TMX-55448
(NASA CR OR TMX OR AD NUMBER)

(THRU)

(CODE)

07
(CATEGORY)

PHASE STABILITY ASPECTS
OF THE GSFC
BORESIGHT RF SOURCES

by

BRUNO W. REICH

7 January 1966

GODDARD SPACE FLIGHT CENTER
Greenbelt, Maryland

CONTENTS

	Page
INTRODUCTION	1
ANALYSIS	1
MEASUREMENTS	4
PROJECTIONS	4

PHASE STABILITY ASPECTS OF THE GSFC BORESIGHT R. F. SOURCES

by

Bruno W. Reich

INTRODUCTION

A recent article by L. R. Malling, Phase Stable Oscillators For Space Communications, including the Relationship between the Phase Noise, the Spectrum, the Short-Term Stability, and the Q of the Oscillator, which appeared in the July 1962 issue of the proceedings of the IRE has brought to light an area of interest concerning the development of the Stable R. F. Sources supplied by Collins Radio. Present day oscillators used in telemetry equipment are not irrefragably stable; however, several obvious examples of instability such as microphonics and power line modulation can be reduced to oblivion by use of solid state devices, carefully smoothed power supplies, and judicious component layout and construction. The resulting oscillator will produce not a monochromatic signal but an orderly noise spectra created by the noise perturbation within the oscillator and associated circuitry. It is the purpose of this paper to determine these values in terms of phase jitter and describe a laboratory technique for measurements.

ANALYSIS

The oscillator may be represented by the equivalent circuit shown in Figure 1, where R_g is the generator resistance, R_θ is the resistance associated with the Phase-Control circuit, R_s is the series resistance of the crystal, and R_e is the emitter Bias resistor. The individual noise currents comprise the total noise power,

$$I_T^2 = i_g^2 + i_\theta^2 + i_s^2 + i_e^2$$

Where i represents the noise current produced by the equivalent circuit resistance.

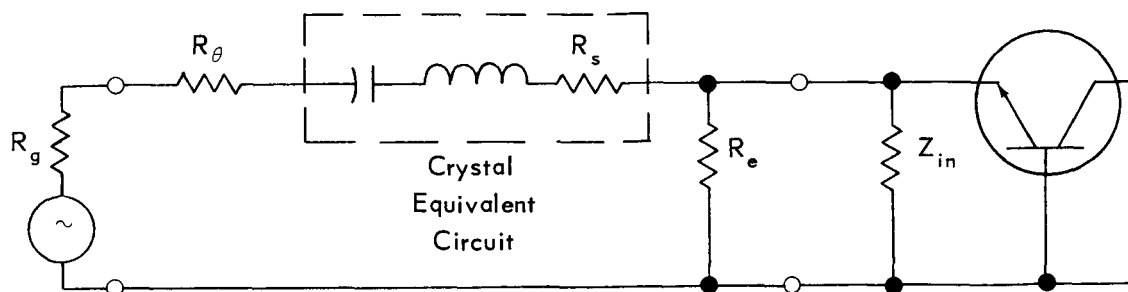


Figure 1

Let us now determine the SNR of a typical 30 mc transistor oscillator. Assuming an in-circuit loaded crystal Q of some 15,000, the noise bandwidth is 3KC. We may further assume a noise figure of 8 db for the transistor and an additional 10 db for the noise attribution of I_T . The total RMS Noise input power is -121dbm.

For a signal input of 50 mv and an input impedance 50 ohms the total RMS signal input power is -14dbm. The signal to noise ratio is now established as 107db, or a voltage ratio of 2.24×10^5 . The expected peak phase jitter may now be related to 1 radian RMS:

$$\text{Peak Phase Jitter} = \frac{1 \text{ Rad RMS} \times \text{Crest Factor} \times 57.3^\circ/\text{Rad}}{2.24 \times 10^5}$$

Assuming a crest factor of 4, $d\phi = .001^\circ$

The frequency of oscillation is determined by the feed back loop of the oscillator circuitry. In a well designed oscillator this is dependent primarily on the crystal. For the small angles considered it may be shown that

$$\frac{d\phi}{df} = \frac{2Q}{f_o}$$

and

$$df = \frac{d\phi \times f_o}{2Q}$$

Based on previous assumptions

$$\begin{aligned} df &= \frac{.001 \text{ degrees} \times 30 \times 10^6 \text{ cps}}{2 \times 15,000 \times 57.3 \text{ degrees/Rad}} \\ &= 0.0167 \text{ cps @ 30 mc} \end{aligned}$$

The oscillator frequency is modulated by thermal noise agitations. This may be described as random-impulse modulation and the resulting sidebands may be predicted based on well known laws of probability and statistics. A random noise sideband analysis will show that a modulation index of 0.66 will produce these hypothetical anti-symmetrical FM sidebands.

$$MI = \phi = \frac{df}{f_m} = 0.66$$

For the case considered, the noise modulation component (f_m) that will produce $df = .0167\text{CPS}$ is:

$$f_m = \frac{.0167}{0.66} = .0253 \text{ CPS}$$

If this assumed oscillator is multiplied by 4.55 to obtain a 136.5 mc source the frequency deviation, and the rate will be increased accordingly to maintain the modulation index of 0.66

Consequently @ 136.5 mc a

$$\begin{aligned} df &= .076 \text{ cps} \\ f_m &= .115 \text{ cps} \end{aligned} \quad \text{and an}$$

will produce peak phase excursions of 0.66 radians, or 38° peak.

If we proceed to measure these phase perturbations with a phase lock loop we may expect the phase noise spectral density to diminish from 0.115 cps at the rate of 6 db per octave. The loop will act as a high pass filter to the phase perturbation and will attenuate the low frequency component below the loop bandwidth at the rate of 6 db per octave.

Consequently the measured phase jitter as a function of loop bandwidth will be expected to diminish at the rate of 12 db per octave.

With a loop bandwidth of 3 cps, the expected phase excursions will be attenuated 3 db due to the $|1-H(s)|$ function and 28.5db due to the $1/S$ function, for a total of 31.5 db or a voltage ratio of 37.6:1. Thus the expected phase jitter @ 3 cps is

$$MI = \frac{.66}{37.6} = .0175 \text{ Rad or } 2^\circ \text{ p-p.}$$

If we employ a scheme of Hetrodyning two 136.5 mc sources within 20 kc and locking on to the resulting signal with a model VIII Interstate tracking filter,

see Figure #2, we have a means to measure the phase jitter as a function of loop bandwidth. Assuming a 300kc free-running oscillator in the tracking filter with an effective in-circuit loaded Q of 150, the expected phase jitter of the measuring device is 0.44 p-p @ α 3 cps loop bandwidth. Hence the measuring device is approximately 5 times better than the device under test and should serve its purpose satisfactorily.

MEASUREMENTS

Data was taken with a camera attached to the scope as shown in Figure 2. It should be noted that the exposure time was 120 seconds, sweep rate of 5 sec/cm, the scope was direct coupled, and a low pass filter @ 10 cps was used to minimize the effects of 60 cps hum inherent in the tracking filter. The results of laboratory performed experiment is shown in Figure 3 with different values of loop bandwidth. To maintain good definition the scope sensitivity was changed accordingly. It should be noted that the experimental results deviate from the predicted performance in the region of 1.0 degrees peak to peak. See Figure 4. It is believed that the inherent 60 cps hum in the Tracking Filter is partly responsible for this deviation. The tracking Filter 60 cycle hum was measured as effectively 4 degrees peak to peak, using the internal calibrate oscillator, which could not be removed entirely by the low pass filter.

As a matter of interest the system was calibrated by phase modulating one of the sources 60° peak to peak, as indicated on the modulation meter, at a 20 cps rate. The scope sensitivity was set for 50 millivolts per centimeter, the loop bandwidth was measured as 5.0 cps, and the scope deflected 6 cm; thus the calibration was 10° per centimeter or 5 millivolts per degree peak to peak.

The differences between the predicted performance and the measured performance may be due to invalid assumptions in the derivation or they may be due to the fact that one of the sources was "pulled" from it's natural frequency of oscillation by 20 kc at the final output frequency. If one can assign an equal contribution of phase jitter to each of the sources then one is at liberty to divide the measured peak to peak phase jitter by a factor of two. Thus the predicted performance is within these two limits.

PROJECTIONS

Based on these predictions at 136 mc, predictions of peak to peak phase jitter as a function of loop bandwidth are made and plotted in Figure 5 for the 400 mc sources, the 1700 mc sources, and for the 2300 mc sources.

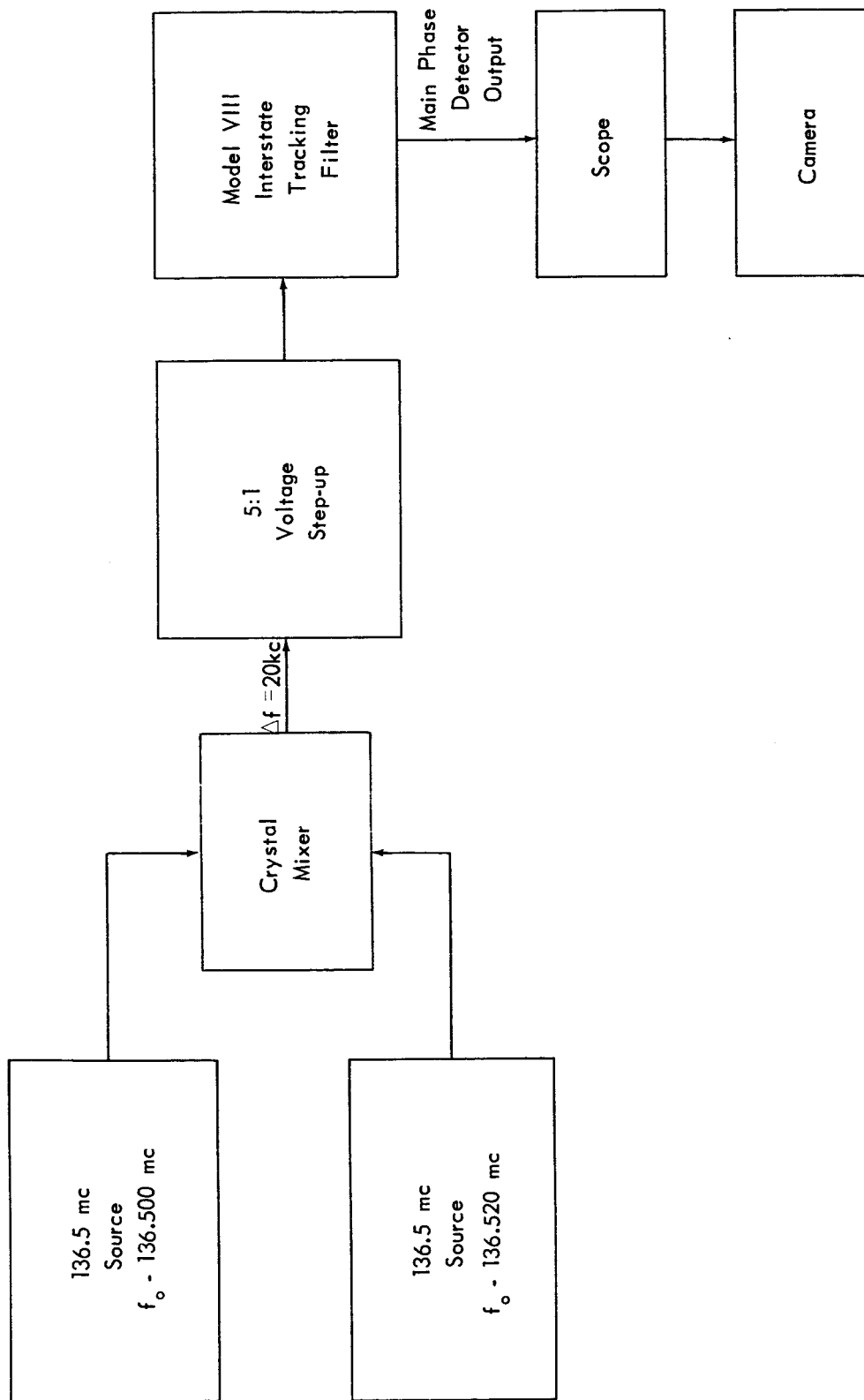
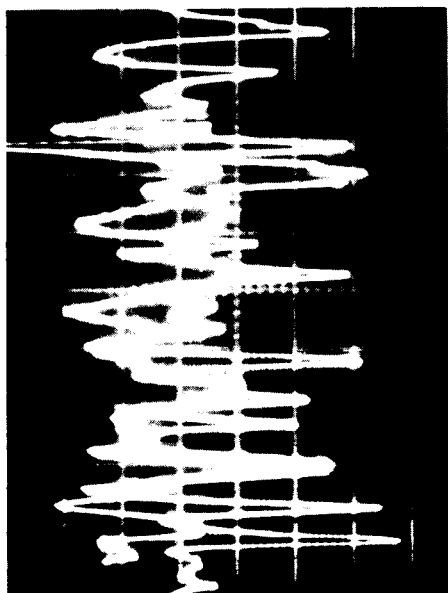
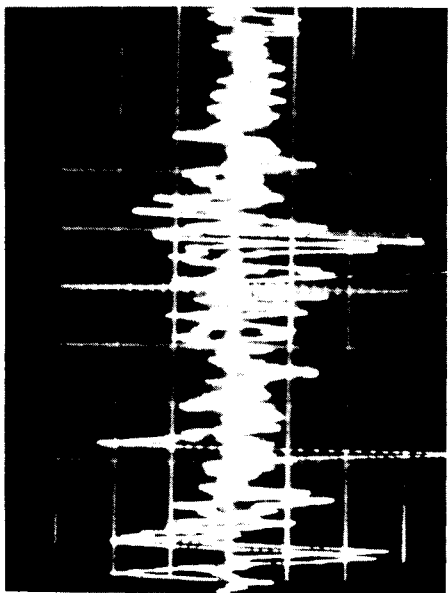


Figure 2. Phase Jitter Measurement Test Set-up



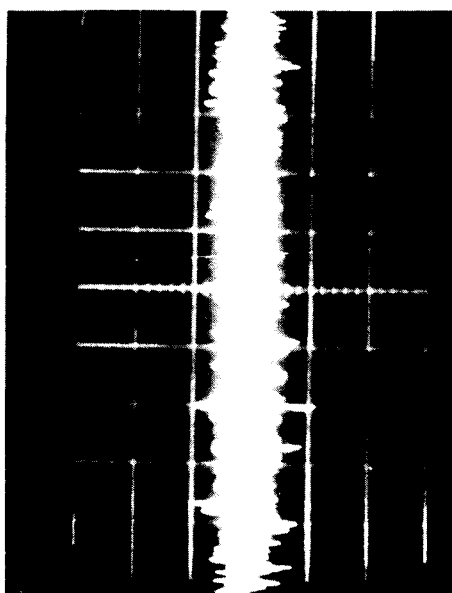
LBW = 0.5 cps 20° p-p/cm
EST - 120° p-p



LBW = 1.0 cps 4° p-p/cm
EST - 24° p-p



LBW = 2.0 cps 1° p-p/cm
EST - 7° p-p



LBW = 5.0 cps 1° p-p/cm
EST - 2° p-p

Figure 3

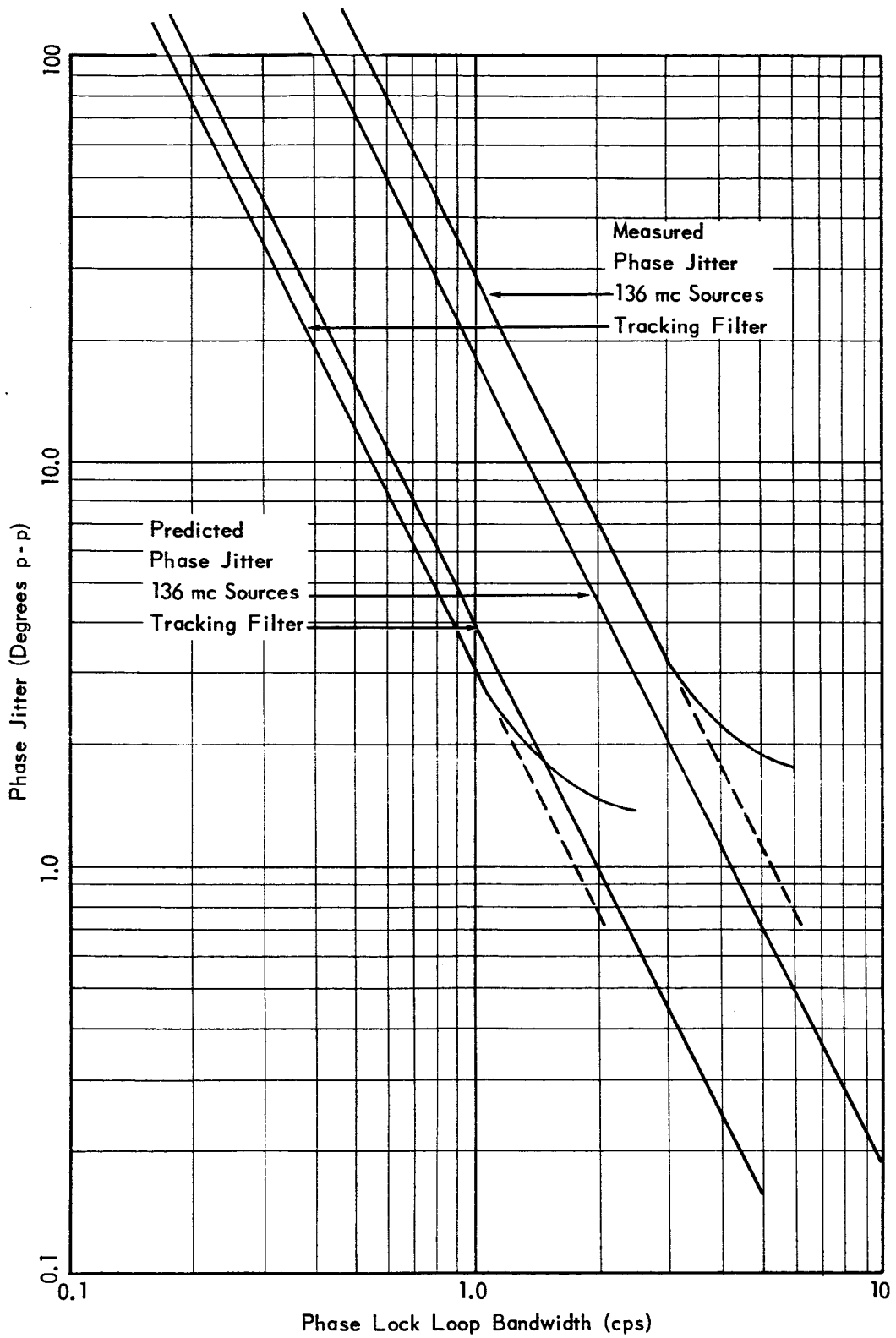


Figure 4

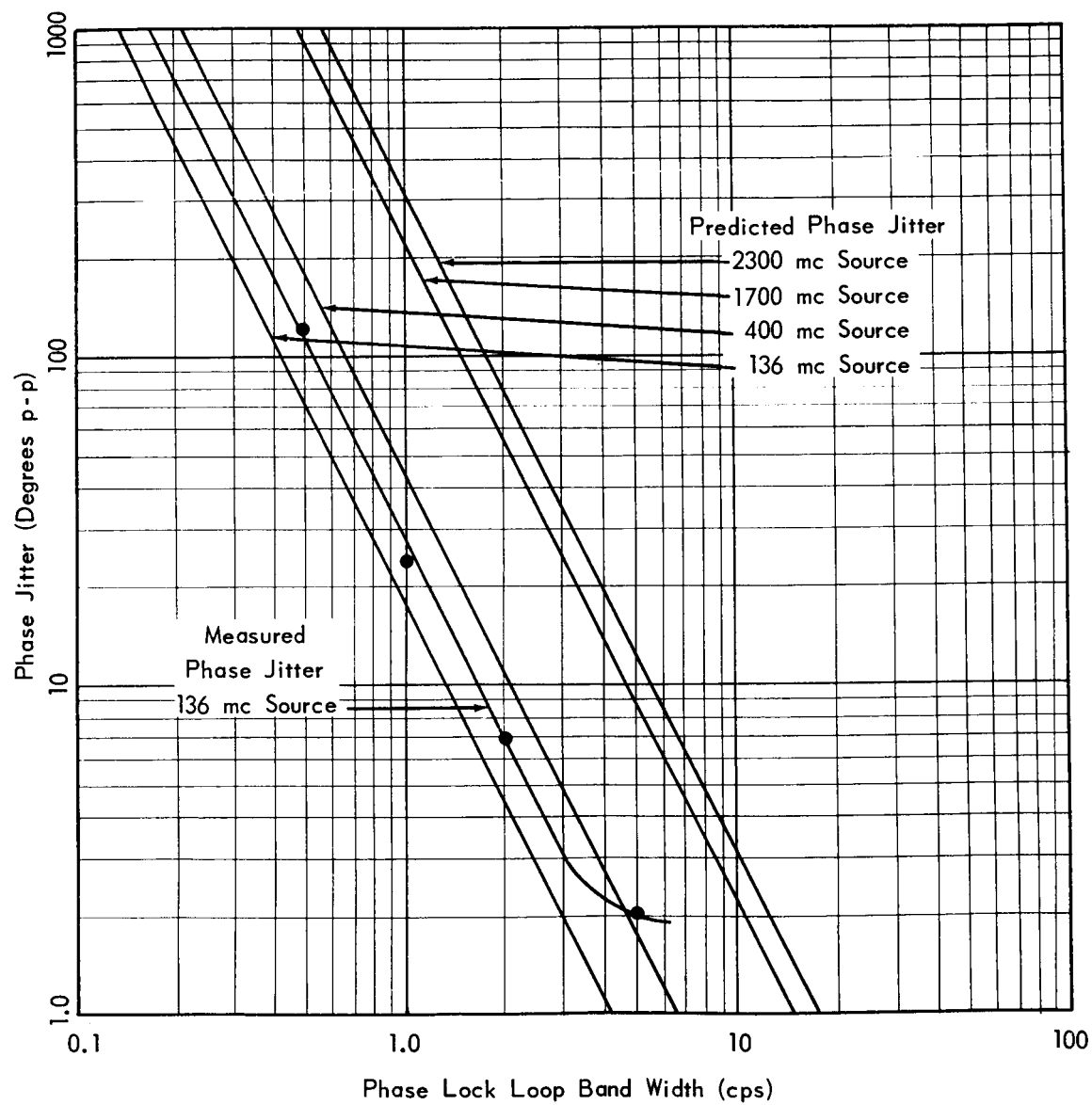


Figure 5